

Appendix

Sequence Data and Alignment

We have used *Drosophila melanogaster* sequence fragments with accession numbers AJ568984-AJ571588 [1], from [2] and AM000058-AM003900 [3]. These fragments are scattered across the X chromosome, and we take only those with sample of 12 individuals from a Zimbabwe population. We then align these fragments to a single *D. simulans* outgroup sequence [1–3]. The aligned loci are binned into five broad genomic categories: 4-fold synonymous sites and nonsynonymous substitutions in protein coding DNA, intergenic regions, introns, and UTRs, using flybase Annotation Release 4.3. If we use the the classification from Releases 4.0 and 3.2 as in refs. 2 and 3, the conclusions of the paper remain unchanged. Altogether we have 271 fragments of data spanning ~ 134 kb of genomic sequence. We have not excluded regions of low recombination from the principal analysis. However, if a cutoff is imposed for the sets [1, 3] with the recombination rate estimates provided in refs. 1 and 3, the results do not change significantly (P values need to be adjusted for the partial linkage as discussed below).

We have used the two programs CLUSTALW1.83 [4] and MLAGAN [5] for multiple alignment of ingroup and outgroup sequences, and we have examined the dependence of the alignment on the scoring parameters. The primary concern is that the count distributions $\hat{Q}(k)$ inferred from the alignment must not overestimate the frequency of substitutions, which may be caused by a too stringent gap score, and thus produce a spurious signal of adaptation. The alignment underlying the counts reported in Table 2 has been obtained by CLUSTALW1.83 with default parameters for coding regions and more relaxed gap opening and extension score for noncoding regions. It fulfils the following consistency criteria: The inferred count distributions do not change significantly (*i*) if the MLAGAN tool with equivalent scoring parameters is used instead, (*ii*) if gap opening and extension cost are scaled down further or (*iii*) if counts are obtained only from the subset of “anchored” loci, where the alignment contains no gaps in a window of 10 bp upstream and downstream.

Table 2. Total number L of loci and numbers of conserved positions ($k = 0$), k -fold single-nucleotide polymorphisms ($k = 1, \dots, 11$), and point substitutions within the sample ($k = 12$).

Category	L	$k = 0$	1	2	3	4	5	6	7	8	9	10	11	12
4-fold syn.	3136	2687	69	38	21	10	9	16	12	6	11	8	10	239
Nonsyn.	14143	13824	49	12	6	3	3	4	6	2	5	1	6	222
Intergenic	59648	55250	932	276	138	104	80	73	57	74	59	64	78	2463
Intronic	47371	43293	751	235	142	92	79	64	65	43	52	60	85	2410
UTRs	10674	10076	99	23	6	9	6	7	6	9	0	3	4	426

Inference of Evolutionary Parameters

Maximum-Likelihood Procedure. The evolutionary parameters reported in Table 1 of the main text are obtained by maximizing the sum of total scores S from all five genomic categories under the fluctuating-selection model, which are given by Eq. 24. The model parameters κ , σ_{ave} , c_s , μ are specific to each category (μ is shared within coding

DNA), the evolutionary time t is a global parameter for all categories. Hence, our procedure neither assumes neutral evolution of 4-fold synonymous sites nor contains other assumptions contained in prior distributions of model parameters. Its consistency is indicated by a number of properties: (i) The maximum-likelihood values of the scaled neutral mutation rate are very similar in all five categories: $\mu = 0.0263$ (4-fold synonymous sites and nonsynonymous changes), $\mu = 0.0334$ (intergenic regions), $\mu = 0.0308$ (introns), and $\mu = 0.0340$ (UTRs). (ii) The maximum-likelihood value of the scaled divergence time, $t = 1.85$, gives $\mu t = 0.048$, and using the independent estimate $\mu = 1.5 \times 10^{-9}$ (per site per generation [6]), this translates into a divergence time $t = 3.2 \times 10^7$ generations = 3.2 million years, in accordance with previous estimates [7]. (iii) The values of t , as well as μ and σ_{ave} for 4-fold sites obtained from a joint fit to all categories are very close to the corresponding values $t = 1.75$, $\mu = 0.0260$ and $\sigma_{\text{ave}} = 1.3$ obtained from 4-fold sites alone. This is nontrivial since this category contains only 2.32% of the loci. (iv) If we assign an equal weight on the different categories (ignoring the fact that we have different total number of sites for each genomic category), we do not observe significant change in the inferred parameter values, indicating that the regions with less data are not compromised by the joint analysis. (v) The inferred level of selection in 4-fold synonymous sites is weak ($\sigma_{\text{ave}} \approx 1$), in accordance with previous results [8]. (We impose the constraint $c_1 = 1$ for this category, since neutral and selected sites cannot be resolved at this low level of selection). (vi) All other categories have substantial maximum-likelihood values of σ_{ave} and of $c_s = 0.94[0.89, 0.97]$ (nonsynonymous changes), $0.80[0.72, 0.85]$ (intergenic regions), $0.76[0.64, 0.91]$ (introns), $0.92[0.89, 0.99]$ (UTRs), in accordance with the substantial deviations of the polymorphism frequency distributions from the form expected at neutrality (see Fig. 2). However, if strong hitchhiking effects are present, these values of c_s rather estimate the combined fraction of sites subject to selection and to hitchhiking (see the discussion below). (vii) The results do not depend on details of the fitness distribution $\Omega(\sigma)$, see below.

In the same way, we obtain the maximum-likelihood neutral model and the best equilibrium model by imposing the global constraints $\sigma_{\text{ave}} = 0$ and $\kappa = 0$, respectively. The demographic model also uses the constraint $\kappa = 0$ and introduces the initial time t_i , the duration $t_f - t_i$, and the scaled strength ν_b of the bottleneck as additional global parameters (for model details, see next section). The obtained maximum-likelihood values are $t_i = 0.0$, $t_f - t_i = 0.65$, $\nu_b = 0.008$. The constrained models use the same value of t as the unconstrained fit, in order to preserve the consistency property (iii) (i.e., to avoid runaway fits with a large overestimation of μt and spurious substantial selection at 4-fold synonymous sites).

Fitness Distributions. In order to infer selection, we have to use a parametrization of the distribution of selection amplitudes $\Omega(\sigma)$ ($\sigma \geq 0$) in a given genomic category. The present dataset imposes a two-fold constraint on this inference: With $m = 12$ individuals in the ingroup species, polymorphism spectra are informative only about a restricted range of selection amplitudes, $\sigma < 50 - 100$. Secondly, there are of order 10^4 loci in a genomic category, so detailed shape characteristics of $\Omega(\sigma)$ cannot be resolved. Within this constraint, we choose distributions so as to be maximally informative of our model. These should contain at least two independent degrees of freedom: (i) the fraction c_s of sites under substantial selection (say, $\sigma > 2$, for which adaptive changes dominate the

Table 3. Selection parameter inference for for the fitness distributions S1, S2, S3.

	c_s			σ_{ave}			κ		
4-fold synonymous	0.0	0.22	0.0	1.4	1.3	1.0	0.0	0.0	0.0
Nonsynonymous	0.94	0.94	0.95	115.	116.	119.	0.12	0.12	0.14
Intergenic	0.80	0.80	0.86	17.	17.	17.	0.27	0.27	0.33
Intronic	0.76	0.76	0.83	14.	14.	14.	0.44	0.45	0.51
UTRs	0.92	0.92	0.95	39.	39.	33.	0.37	0.39	0.42

sequence turnover as given by $\tilde{\alpha} > 1/2$ in Eq. 17) versus the fraction of sites under weak selection (for which background changes dominate, $\tilde{\alpha} < 1/2$), and (ii) the average level of selection σ_{ave} . Specific forms used include a sum of two delta functions,

$$\Omega(\sigma) = Z^{-1}[(1 - c_1)\delta(\sigma) + c_1\delta(\sigma - c_2)], \quad [\text{S1}]$$

a sum of two Gaussians,

$$\Omega(\sigma) = Z^{-1}[(1 - c_1)\exp(-2(\sigma^2)) + c_1\exp(-(\sigma - c_2)^2/3)], \quad [\text{S2}]$$

and two facing exponentials

$$\Omega(\sigma) = \begin{cases} Z^{-1}[(1 - c_1)\exp(-\sigma/3)/3 + c_1\exp(-(c_2 - \sigma)/3)/3] & (\sigma \leq c_2), \\ 0 & (\sigma > c_2) \end{cases} \quad [\text{S3}]$$

with appropriate normalization factors Z^{-1} and two basic parameters c_1, c_2 , which can be expressed in terms of c_s and σ_{ave} . Our inference procedure satisfies the following criteria: (i) The two-parameter form is statistically significant, i.e., the single-parameter restriction given by the constraint $c_1 = 1$ is less likely with $P < 10^{-11}$ in all categories except 4-fold synonymous sites. (ii) Within the two-parameter forms (Eqs. S1-S3), the inferred selection characteristics do not depend significantly on the type of parametrization used (see Table 3) nor on further details which cannot be resolved, e.g., the width of the Gaussians in Eq. S2 or of the exponentials in Eq. S3. (iii) Adding further independent parameters to $\Omega(\sigma)$ does not increase the maximum likelihood and does not lead to inconsistencies. In particular, the data are consistent with the assumption that a fraction of the sites has selection strengths outside our inference region ($\sigma > 100$), and this assumption increases σ_{ave} but does not affect the inferred value of κ .

Estimation of P values and Confidence Intervals. Our procedure produces the maximum-likelihood score $S^* = 4082$ for the fluctuating-selection model, and significantly smaller values $S' = 3814$ (neutral model), $S' = 3951$ (equilibrium model), and $S' = 4008$ (demographic model). The P values of observing the data under one of the alternative models is given by

$$P \equiv \text{Prob}(S > S^*) \sim \exp(-c \Delta S) \quad [\text{S4}]$$

in terms of the score difference $\Delta S \equiv S^* - S'$. The constant takes the value $c = 1$ for independent loci, but is modified in the dataset by partial linkage between loci. To quantify this effect, we have simulated the evolution of a population of sequences with

recombination. The scaled recombination rate is chosen such that the distance-dependent correlation between polymorphic sites as measured by the Hill-Robertson coefficient [10] matches that of the dataset, leading to levels of $\rho \approx 0.1$ in accordance with previous results [3]. This model produces a score distribution whose tail is of the form Eq. S4 with $c \approx 0.35$. For the p -values reported in the main text we further discount for model complexity in the Akaike Information Criterion sense by subtracting the difference of free parameters between the compared models from the score difference $c \Delta S$. The confidence intervals around the maximum-likelihood parameters appearing in Table 1 are obtained in a standard way by sampling from their Bayesian posterior distribution.

Comparison with Population-Genetic Tests. The above P values can be used for a quantitative comparison with other tests for adaptive selection. For a set of allele counts drawn from an input distribution Q , the difference of scores Eq. 24 between Q and an alternative model Q' , normalized per locus, has a simple probabilistic interpretation as the relative entropy or Kullback-Leibler distance $D(Q, Q')$ of the distributions Q and Q' ,

$$\Delta s \equiv \frac{\Delta S}{L} = D(Q, Q') \equiv \sum_k Q(k) \log \left(\frac{Q(k)}{Q'(k)} \right). \quad [\text{S5}]$$

In particular, it is independent of the reference distribution Q_0 in Eq. 24. Consider now a coarse-grained distribution Q_{cg} of Q , which is defined by summing any subset(s) of entries $Q(k)$, resulting in a smaller number of new entries $Q_{\text{cg}}(\tilde{k})$ ($\tilde{k} = 0, \dots, \tilde{m}$), and the analogous coarse-grained distribution Q'_{cg} of Q' . It is straightforward to show that any coarse-graining leads to a loss in relative entropy, $D(Q_{\text{cg}}, Q'_{\text{cg}}) \leq D(Q, Q')$, i.e., to a less significant P value. The allele frequency information underlying the standard population genetic tests for adaptation can be seen as such coarse-grainings of the full distributions used here.

(i) The coarse-graining Q_{MK} underlying the McDonald-Kreitman test has three entries,

$$Q_{\text{MK}} \equiv \left\{ Q(0) = 1 - Q^p - Q^s, \quad Q^p = \sum_{k=1}^{m-1} Q(k), \quad Q^s = Q(m) \right\}. \quad [\text{S6}]$$

Adaptive evolution is inferred if $Q^s Q_0^p / Q^p Q_0^s > 1$, where Q_0^p and Q_0^s are the polymorphism and substitution frequencies in a neutral reference class. If we assume that the evolutionary time $t = Q_0^s / Q_0^p$ has been inferred correctly from the neutral class, the McDonald-Kreitman test is equivalent to a maximum-likelihood procedure for the coarse-grained distribution Q'_{MK} with the equilibrium constraint $\kappa = 0$ and with t taken from the input model Q . The resulting score differences

$$\Delta s_{\text{MK}} = D(Q_{\text{MK}}, Q'_{\text{MK}}) \quad [\text{S7}]$$

then provide a quantitative comparison with our procedure, as shown in Fig. 2(a,b) of the Main Text. In particular, it is straightforward to show that $\Delta s_{\text{MK}} = 0$ iff $Q^s Q_0^p / Q^p Q_0^s \leq 1$, which defines the parameter region where the McDonald-Kreitman test does not infer adaptations (marked by stripes in Fig. 2(b,d) of the Main Text).

(ii) Similarly, the inference methods using only information from the relative frequencies of polymorphisms, such as Tajima's D test [11], can be derived from the coarse-graining

$$Q_{\text{poly}} \equiv \left\{ Q(0) + Q(m) = 1 - Q^p, \quad Q(1), \dots, Q(m-1) \right\} \quad [\text{S8}]$$

with $Q^p = \sum_{k=1}^{m-1} Q(k)$. We can again perform a maximum-likelihood procedure for the coarse-grained distribution Q'_{poly} with the equilibrium constraint $\kappa = 0$. Variation of μ will reproduce the input value of Q^p , and the maximum-likelihood score difference depends only on the shape difference of the polymorphism spectra as given by the normalized distributions $q_{\text{poly}} \equiv \{Q(1)/Q^p, \dots, Q(m-1)/Q^p\}$ and q'_{poly} ,

$$\Delta s_{\text{poly}} = D(Q_{\text{poly}}, Q'_{\text{poly}}) = Q^p D(q_{\text{poly}}, q'_{\text{poly}}) + O(\mu^2). \quad [\text{S9}]$$

Although adaptive evolution can be inferred for all $\sigma, \kappa > 0$, there is again a substantial loss in significance compared to the full distributions as shown in Fig. 5.

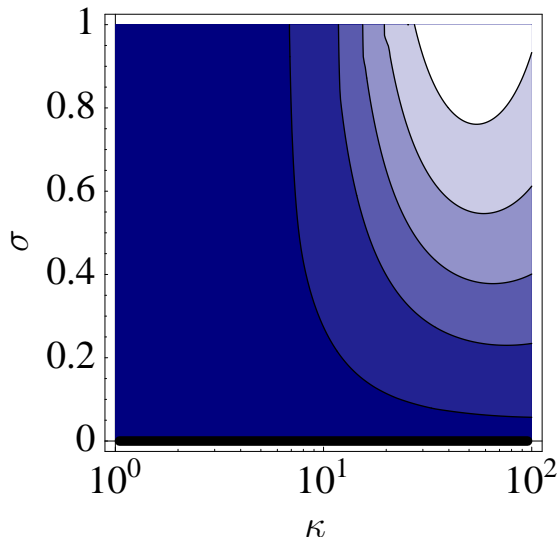


Fig. 5. Inference of adaptive evolution from polymorphism spectra, to be compared with Fig. 2 a and b. Statistical evidence for adaptation, as given by the likelihood score difference per locus, Δs_{poly} , between the input model and the best equilibrium ($\kappa=0$) model as a function of the input selection parameters σ and κ (input μ and t as in the *Drosophila* datasets). Contours from bottom to top: 0 (thick line), 5×10^{-6} , 5.5×10^{-5} , 1.5×10^{-4} , 2.0×10^{-4} , 2.5×10^{-4} (thin lines).

Model Generalizations

The model (1) has the advantage of allowing for explicit analytical predictions of allele frequency distributions, so that the analysis of genomic data can be based on a systematic probabilistic analysis. However, a number of features present in genomic data are not covered by this model. Here we demonstrate by analytical and numerical analysis that these do not affect the conclusions of this paper.

Varying Neutral Mutation Rates. The neutral rates $\mu_{a \rightarrow b}$ for nucleotide point substitutions vary by factors of order 1, depending on the type of process (transition or transversion), the neighboring nucleotides, the *GC*-content of the flanking region etc. Differences in the average neutral rate μ between genomic categories are taken into account by our maximum-likelihood parameter inference. Here we consider a bias in the neutral

Table 4. Parameter inference for models with mutation rate bias ($\mu_{a \rightarrow b} = 1.5\mu_{b \rightarrow a}$) (M) or with four alleles (F1, F2, F3), see text.

Input model					ML fit	
Type	σ		κ		σ_{ml}	κ_{ml}
M	6		0		6.1	0.0
M	12		0		11.9	0.0
M	6		0.5		6.4	0.47
M	12		0.5		12.1	0.53
Type	σ_{21}	σ_{31}	σ_{41}	κ	σ_{ml}	κ_{ml}
F1	0	0	6	0.0	5.8	0.02
F1	0	0	12	0.0	12.	0.01
F2	0	6	6	0.0	3.3	0.06
F2	0	12	12	0.0	3.8	0.05
F3	6	12	18	0.0	9.1	0.01
F3	12	24	36	0.0	16.	0.01
F1	0	0	6	0.5	5.5	0.45
F1	0	0	12	0.5	9.9	0.65
F2	0	6	6	0.5	3.9	0.43
F2	0	12	12	0.5	4.5	0.56
F3	6	12	18	0.5	9.2	0.53
F3	12	24	36	0.5	18.	0.69

The inferred maximum-likelihood parameters σ_{ml} , κ_{ml} using the two-allele standard model are a good approximation of the corresponding (average) values of the input model. In particular, there is no spurious inference of $\kappa > 0$.

rate between the forward and backward substitutions, $\mu_{a \rightarrow b} = 1.5\mu_{b \rightarrow a}$, corresponding to a nucleotide frequency bias $\lambda_{\text{eq}} = 0.4$ at equilibrium. We obtain numerically the distribution functions $p(x, t)$ and $p'(x, t)$ of the biased Fisher-Wright process along the two phylogenetic branches, subsequently averaging over initial conditions at the speciation point and over many realizations of the Poisson process of selection. The recorded outgroup directed count distribution $\hat{Q}(k)$ is then subject to the parameter inference using Eq. (20), which is based on the unbiased model (1). The inferred maximum-likelihood parameters σ_{ml} and κ_{ml} are consistent with the true input parameters σ and κ , as shown in Table 4.

Four-Allele Loci. A similar potential confounding factor arises from the fact that a single-nucleotide genomic locus has four alleles (A, C, G, T), allowing for three independent selection coefficients and a richer scenario of selection fluctuations than our basic model. We obtain numerical distributions $\hat{Q}(k)$ for three variants (F1, F2 and F3) of the four-allele model: a single preferred nucleotide ($\sigma_{ab} = \sigma_{ac} = \sigma_{ad} > 0$), two preferred nucleotides of equal fitness ($\sigma_{ab} = 0, \sigma_{ac} = \sigma_{ad} > 0$), and three different fitness values ($\sigma_{ab} \neq \sigma_{bc} \neq \sigma_{cd} > 0$), with fluctuations acting as random permutations of the nucleotide fitness values with rate $\kappa\mu$. The maximum-likelihood selection parameters σ_{ml} and κ_{ml} shown in Table 4 are seen to provide good estimates of the average magnitude σ and the rate κ of the input model.

Nonrandom Samples. A sample from a limited geographical region may have a smaller coalescence time t_c to its last common ancestor than a true random sample, where $t_c \approx 1$ in our rescaled units. The outgroup-directed allele frequency distribution $\hat{Q}(k)$ for an ingroup sample with $t_c = 0.5$ is obtained by propagating the solution of the Master equation on the

ingroup branch for a time $t - t_c$, drawing the allele of the sample ancestor, and propagating the allele frequency distribution for its descendants for a time t_c . This distribution shows a reduced level of polymorphisms with large values of k already for neutral evolution, leading to poorer fits with the model distributions $Q(k)$ for random samples. The genomic count distribution $\hat{Q}(k)$ for 4-fold synonymous sites does not show reduced frequencies of large- k polymorphisms with respect to the distribution $Q_0(k)$ under neutral evolution given by (20) (see Fig. 3), indicating that the data used in this study are indeed a good random sample.

Demographic Effects. We consider the evolution with a time-dependent ingroup population $N(t) = \nu(t)N$ of the form

$$\nu(s) = \begin{cases} 1 & 0 \leq s < t_i, \\ \nu_b & t_i \leq s < t_f, \\ 1 & t_f \leq s \leq t, \end{cases} \quad [\text{S10}]$$

where $t = 0$ is the speciation point and t is the divergence time. Our maximum-likelihood inference of the bottleneck model is based by numerical integration of the Fokker-Planck equation. Bottlenecks which do not affect the polymorphism spectrum ($t - t_f > 1$) can also be treated using the quasistationary approximation (10) piecewise for the time intervals of constant ν , with scaled selection coefficients $\sigma(t) = \sigma\nu(t)$. The validity of this approximation is shown in Fig. 6, where we compare the analytical prediction for the sequence divergence g_{+-} with the numerical solution.

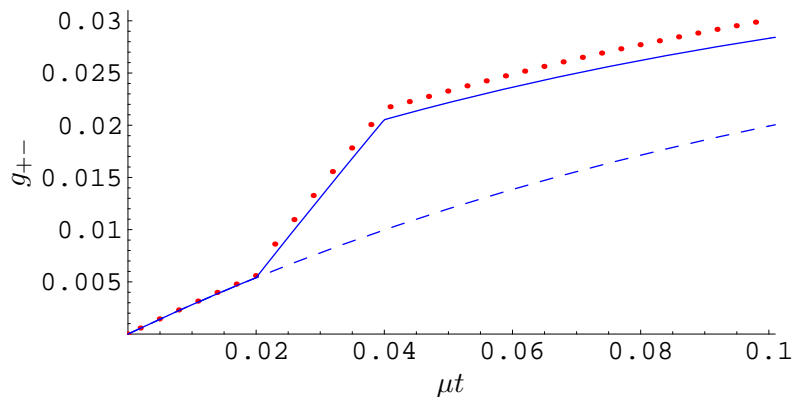


Fig. 6. Sequence divergence under time-dependent population size. The divergence g_{+-} given by (18) is plotted against μt for evolution under stationary selection ($\kappa = 0$) of strength $\sigma = 4$ (solid line), with a bottleneck with parameters $t_i = 0.02$, $t_f = 0.04$, $\nu_b = 0.2$ on the ingroup branch and without a bottleneck (dashed line). Analytical curves are obtained using the quasistationary approximation, data points by propagating the distribution $p(x, t)$ using the exact continuous-time Master equation.

Linkage Between Loci, Hitchhiking. We estimate the hitchhiking parameter ω given by Eq. 25 for the selected categories with Φ values from Table 1 and a conservative value $\rho = 0.05$ as obtained above. The resulting ω values are of order 1, suggesting that hitchhiking effects cannot be excluded. To address this issue, we have simulated

the evolution of partially linked loci for $\rho = 0.05$ and different values of κ , c_s , σ_{ave} , and have measured the influence of hitchhiking on the allele frequency distribution $\hat{Q}(k)$ and the inferred parameters (see Table 5). As expected, the allele frequency distribution at neutral loci shows a depletion of intermediate-frequency polymorphisms [9]. This can affect parameter inference from the standard model of independent loci: c_s is overestimated, but the fitness flux $\Phi \simeq \omega\rho$ is reproduced more faithfully. At the inferred level of ω , these effects are weak, leading to a self-consistent prediction. However, we cannot exclude that actual values of ω are somewhat higher, which would imply that the inferred parameters reported in Table 1 are lower bounds but would leave the conclusions unaffected.

Integrals

Here we explicitly write down the integrals needed in the *Main Text*. The normalizing factor for elementary solutions p_a in Eq. 4 reads

$$Z_a = \frac{\Gamma(\mu)^2}{\Gamma(2\mu)} [1 - e^{-a\sigma} {}_1F_1(\mu, 2\mu, a\sigma)], \quad [\text{S11}]$$

where Γ is Euler's Gamma function and ${}_1F_1$ is Kummer's confluent hypergeometric function. The moments Eq. 21 are

$$M_a^\epsilon(k, m) = \begin{cases} \binom{m}{k} Z_\epsilon^{-1} \frac{\Gamma(k+\mu)\Gamma(m-k+\mu)}{\Gamma(m+2\mu)} [1 - e^{-\epsilon\sigma} {}_1F_1(k + \mu, m + 2\mu, \epsilon\sigma)] & (a = 1) \\ \binom{m}{m-k} Z_\epsilon^{-1} \frac{\Gamma(m-k+\mu)\Gamma(k+\mu)}{\Gamma(m+2\mu)} [1 - e^{-\epsilon\sigma} {}_1F_1(m - k + \mu, m + 2\mu, \epsilon\sigma)] & (a = -1). \end{cases} \quad [\text{S12}]$$

References

- [1] Glinka, S., Ometto, L., Mousset, S., Stephan, W. & De Lorenzo, D. (2003) *Genetics* **165**, 1269-1278.
- [2] Andolfatto, P. (2005) *Nature* **437**, 1149-1152.
- [3] Ometto, L., Glinga, S., De Lorenzo, D. & Stephan, W. (2005) *Mol. Biol. Evol.* **22**, 2119-2130.
- [4] Chenna, R., Sugawara, H., Koike, T., Lopez, R., Gibson, T.J., Higgins, D.G. & Thompson, J.D. (2003) *Nucleic Acids Res.* **31**, 3497-3500.
- [5] Brudno, M., Do, C., Cooper, G., Kim M.F., Davydov, E., Green, E.D., Sidow, A., & Batzoglou, S. (2003) *Genome Research* **13(4)**, 721-731.
- [6] Li, W. H. (1997) *Molecular Evolution* (Sinauer, Sunderland).
- [7] Caccone, A., Amato G.D. & Powell J.R. (1988) *Genetics* **118**, 671-683.
- [8] Akashi, H. (1995) *Genetics* **139**, 1067-1076.
- [9] Fay, J. C. & Wu, C-I. (2000) *Genetics* **155**, 1405-1413.
- [10] Hill, W. G. & Robertson, A. (1968) *Theor. App. Gen.* **38**, 226-231.
- [11] Tajima, F. (1989) *Genetics* **123**, 585-595.

Table 5. Parameter inference for sequences evolving under fluctuating selection with parameters κ , c_s , σ_{ave} and recombination with rate $\rho = 0.05$.

Input model				ML fit			
κ	c_s	σ_{ave}	Φ	κ_{ml}	$c_{s,\text{ml}}$	$\sigma_{\text{ave,ml}}$	Φ_{ml}
0.20	0.60	9.	0.04	0.16	0.72	10.	0.04
0.30	0.60	9.	0.07	0.23	0.70	12.	0.07
0.40	0.60	9.	0.09	0.40	0.76	11.	0.11
0.50	0.60	9.	0.11	0.51	0.76	11.	0.14
0.20	0.80	12.	0.06	0.21	0.86	13.	0.07
0.30	0.80	12.	0.09	0.29	0.86	14.	0.10
0.40	0.80	12.	0.12	0.35	0.84	14.	0.12
0.50	0.80	12.	0.15	0.45	0.84	12.	0.13
0.20	0.60	15.	0.08	0.24	0.76	15.	0.09
0.30	0.60	15.	0.11	0.32	0.76	15.	0.12
0.40	0.60	15.	0.15	0.30	0.72	19.	0.15
0.50	0.60	15.	0.19	0.63	0.85	13.	0.21
0.20	0.80	20.	0.10	0.18	0.85	22.	0.10
0.30	0.80	20.	0.15	0.28	0.85	26.	0.18
0.40	0.80	20.	0.20	0.42	0.87	20.	0.21
0.50	0.80	20.	0.25	0.50	0.87	23.	0.29
0.20	0.60	21.	0.11	0.18	0.73	20.	0.09
0.30	0.60	21.	0.16	0.35	0.76	21.	0.18
0.40	0.60	21.	0.21	0.45	0.77	20.	0.23
0.50	0.60	21.	0.26	0.56	0.79	22.	0.30
0.20	0.80	28.	0.14	0.23	0.89	25.	0.15
0.30	0.80	28.	0.21	0.31	0.89	30.	0.23
0.40	0.80	28.	0.28	0.38	0.87	31.	0.30
0.50	0.80	28.	0.35	0.48	0.88	31.	0.37
0.20	0.60	27.	0.13	0.18	0.77	34.	0.15
0.30	0.60	27.	0.20	0.32	0.79	27.	0.22
0.40	0.60	27.	0.27	0.43	0.81	27.	0.28
0.50	0.60	27.	0.34	0.52	0.83	31.	0.40
0.20	0.80	36.	0.18	0.18	0.88	45.	0.20
0.30	0.80	36.	0.27	0.31	0.91	39.	0.30
0.40	0.80	36.	0.36	0.35	0.89	44.	0.38
0.50	0.80	36.	0.45	0.47	0.90	38.	0.45
0.20	0.60	33.	0.17	0.20	0.74	33.	0.17
0.30	0.60	33.	0.25	0.28	0.75	34.	0.24
0.40	0.60	33.	0.33	0.47	0.80	25.	0.30
0.50	0.60	33.	0.41	0.55	0.82	31.	0.42
0.20	0.80	44.	0.22	0.18	0.86	44.	0.19
0.30	0.80	44.	0.33	0.32	0.89	40.	0.32
0.40	0.80	44.	0.44	0.39	0.89	42.	0.41
0.50	0.80	44.	0.55	0.52	0.92	36.	0.47
0.20	0.60	39.	0.20	0.26	0.77	27.	0.18
0.30	0.60	39.	0.29	0.31	0.76	35.	0.27
0.40	0.60	39.	0.39	0.45	0.81	33.	0.37
0.50	0.60	39.	0.49	0.53	0.81	31.	0.41
0.20	0.80	52.	0.26	0.18	0.87	57.	0.26
0.30	0.80	52.	0.39	0.29	0.88	50.	0.36
0.40	0.80	52.	0.52	0.40	0.91	52.	0.51
0.50	0.80	52.	0.65	0.42	0.89	59.	0.63

Depending on the parameter $\omega = \Phi/\rho$, the inferred maximum-likelihood parameters using the two-allele standard model can be affected by hitchhiking, which leads to overestimation of c_s .